THE JOURNAL OF CHEMICAL PHYSICS VOLUME 56, NUMBER 12 15 JUNE 1972

Photoionization and Autoionization of H_2

GILBERT B. SHAW* AND R. STEPHEN BERRY

Department of Chemistry and *the James Franck Institute, The University of Chicago, Chicago, Illinois 60637*

(Received 14 January 1972)

The cross sections are calculated for direct photoionization and photoexcited autoionization of H_2 for light in the region 600–800 Å. Angular distributions of directly produced photoelectrons, lifetimes for vibrationally induced autoionization, some spectral assignments, and relative intensities of photoelectrons of various energies (from autoionizing states) are also given. The method by which the Rydberg and continuum state wavefunctions are derived is similar to the correlated pseudopotential method of Tully. The results indicate that correlation has only a small effect on the differential and total cross sections for photoionization. Agreement of theoretical and experimental lifetimes for autoionization is improved by the inclusion of correlation in the wavefunction. Critical tests of the calculations could be made by experimental study of the photoelectron spectra produced when H_2 is excited to certain specific autoionizing states; for these states, the theory predicts anomalously efficient autoionization associated with transfer of *two* vibrational quanta into electronic excitation.

I. INTRODUCTION

We present here a theoretical treatment of the direct photoionization and the vibrationally induced autoionization of the hydrogen molecule, excited by radiation in the region 600–800 Å. There have been theoretical studies of particular aspects of this prototype problem for molecular photoionization: calculations have been made of the total cross section for direct ionization as a function of the wavelength of the incident light,[1,2] of the lifetimes and linewidths of the vibrationally autoionizing states,[3–6] and of the angular distribution of photoelectrons from direct ionization.[7] The theory of rotationally induced autoionization has also been studied recently.[8]

The results of these studies correspond moderately well with experimental findings in some cases, e.g., in the identification and interpretation of widths of the rotationally autoionizing Rydberg states[9] and of the lifetimes of quite a number of vibrationally autoionizing states.[10–12] The agreement between theoretical and experimental cross sections[13,14] for direct photoionization is difficult to assess because of the many autoionizing states that contribute to the total cross section for ionization. Furthermore, the assignment of some of the autoionization peaks in the high-resolution photoionization spectrum[10–12,15] of H_2 may be ambiguous in view of the very high density of spectral lines in the 600–800 Å region.[16–18] It would be desirable to have a theoretical guide for assigning the autoionizing states, in order to test the current theory of molecular autoionization, particularly of vibrationally induced autoionization.

Furthermore, there has been no prior attempt to develop a theoretical analysis of the relative intensities of direct and autoionizing transitions in molecular photoionization. There has been no analysis yet of the role of electron correlation in photoionization, and particularly of the effect of correlation on the angular distribution of photoelectrons. All of these aspects of the problem have been drawn together in the treatment which follows.

We have developed a treatment of photoionization of H_2 which is designed to reflect at least the short-range part of the electron correlation, to give the cross sections for both direct ionization and vibrationally induced autoionization, to determine the angular distribution of photoelectrons from direct ionization and the lifetimes of autoionizing states when electron correlation is included, and to give the energies of autoionizing states with sufficient accuracy to permit the assignment of the observed peaks in the photoionization spectrum of H_2. Two aspects of the total problem have not been included in the present work. These are the angular distributions of electrons from autoionizing states and the shapes (rather than just the widths) of the autoionization peaks.

The treatment has been carried out in the spirit of the many-body pseudopotential method,[19] albeit without the use of the variation method or the "smallest pseudofunction" criterion to optimize the choice of pseudopotential.[19,20] Preliminary calculations were carried out in which the Kohn variation method was used to determine the wavefunction. The photoionization cross sections obtained by fixing the pseudopotential variationally were essentially the same as those obtained by simple orthogonalization. By incorporating the condition that high-energy states must be orthogonal to states of lower energy having the same symmetry and multiplicity, one forces the high-energy wavefunctions to have shapes and nodal structures that reflect this orthogonality. If the wavefunctions of lower energy are many-body functions incorporating electron correlation, then the orthogonalizing procedure automatically includes electron correlation into the total wavefunctions for the high-energy states. The correlation so introduced extends only to distances comparable to the size of the low-energy functions. However Tully's analysis of this method[19] indicates that the short-range correlation

(rather than the long-range polarization part) is by far the larger contributor to phase shifts of low-lying continuum functions and therefore is presumably the more important factor in high Rydberg states as well.

The work discussed here has one further goal, of providing a comparison sufficiently stringent to test other, more approximate theoretical models. Here, the desideratum is determining how much one can expect to rely on the more approximate methods, when molecules more complex than H_2 are investigated.

The next section describes the method by which the calculations were made. The third section presents the results and compares them with experimental results and the findings of other theoretical treatments.

II. METHOD

The calculations of photoexcitation and photoionization were carried out in the electric dipole approximation, and in the dipole length form, so that, for example, the direct photoionization cross section takes the form,[21]

$$\sigma_{i,f}=(8\pi^3\nu/3c)\,(\omega_i)^{-1}\sum|\langle u_i\,|\,D^{k,x}\,|\,u_f\rangle|^2. \quad (1)$$

Here, ν is the frequency of the exciting light, ω_i is the degeneracy of the initial state i (apart from spin degeneracies), u_i and u_f are the wavefunctions for the initial and final molecular states, and $D^{k,x}$ is the dipole operator. This operator takes the form

$$D^{k,x}=-(Ae\nu/mc)\sum_\alpha(\mathbf{x}\cdot\mathbf{r}_\alpha), \quad (2)$$

where A is the field amplitude, $\mathbf{x}$ is the unit polarization vector of the field, and $\mathbf{r}_\alpha$ is the coordinate vector of electron α.

The differential cross section $\sigma_{i,f}(\Omega)$ for photoionization of a randomly oriented ensemble of H_2 molecules was previously developed as a specific example for molecular photoionization,[7]

$$\sigma_{i,f}(\Omega)=(4\pi^2\nu/15c)\{[|\,D^{k,z}\,|^2+|\,D^{k,x+iy}\,|^2 -2\,\mathrm{Re}(D^{k,z*}D^{k,x+y})]+[2\,|\,D^{k,z}\,|^2+7\,|\,D^{k,x+iy}\,|^2 +6\,\mathrm{Re}(D^{k,z*},D^{k,x+iy})]\cos^2\theta\}. \quad (3)$$

The calculation of wavefunctions is naturally the major part of the effort in a problem such as this one. It would have been possible to use either a close coupling method[22] or a polarized orbital method[23,24] to introduce correlation into the wavefunctions. However the success and apparent relative ease of the pseudopotential method introduced by Tully prompted us to use this viewpoint. It was our original expectation that computational advantages would lead us to solve the pseudopotential equation for the unknown two-particle function $\Psi(1,2)$,

$$\int\phi(1)\mathcal{H}\Psi(1,2)+\sum_i\alpha_i(E_i-E)\int\phi(1)\Psi_b{}^i(1,2) =E\int\phi(1)\Psi(1,2), \quad (4)$$

TABLE I. Effect of projection on dipole matrix elements.

E(a.u.)	Symmetry	d(unprojected)	d (projected)
0.004	$^1\Pi_u$	1.35	1.33
0.04	$^1\Pi_u$	0.835	0.825
0.08	$^1\Pi_u$	0.507	0.499
0.20	$^1\Pi_u$	0.345	0.388
0.001	$^1\Sigma_u$	1.99	2.01
0.01	$^1\Sigma_u$	1.67	1.69

where the singlet function $\Psi(1,2)$ is an antisymmetrized product of a bound $1s\sigma_g$ orbital ϕ and an excited Rydberg or continuum function ψ, so that its spatial part has the symmetric form,

$$\Psi(1,2)=2^{-1/2}[\phi(1)\psi(2)+\phi(2)\psi(1)]. \quad (5)$$

As it turned out, it was convenient to solve (4) with all α's equal to zero, and then carry out the orthogonalization to the lower bound states $\Psi_b{}^i$ after finding the function Ψ. The two procedures are entirely equivalent in their results, if one fixes α_i at unity. It should be recalled that the form (4) was introduced as an alternative to orthogonalization in order to remove oscillations from the core region of the unknown function and thus to facilitate computation. However the method we have used loses the flexibility associated with adjustable α's .(Fixing α variationally did not affect the photoionization cross section in preliminary calculations.)

The function $\psi(2)$ was determined by solving Eq. (4) in elliptical coordinates, $\lambda=(r_1+r_2)/R$ and $\mu=(r_1-r_2)/R$, with the dependence on the coordinate μ expanded in spherical harmonics,

$$\psi(2)=(\lambda_2{}^2-1)^{m/2}\sum_j{}^j C_j\Gamma_j(\lambda_2)\,P_j{}^m(\mu_2). \quad (6)$$

Note that m is a good quantum number and that, because H_2 is homonuclear, only odd or even j's appear. Note also that as $r\to\infty$, $\mu\to\cos\theta$ and ψ becomes a conventional expansion in spherical harmonics. At the same limit, $\lambda_2\to 2r/R$, so that ψ is asymptotically given by a conventional partial wave expansion.

An analysis[25] of the partial-wave composition of scattering states of electrons by H_2 showed that a moderately good representation of the scattering state is obtained when only a very few partial waves are included at large r, but that many partial waves enter into the function in the core region. We took this as a guide that a similar situation would occur in the states of e-$H_2{}^+$. This viewpoint has been the basis for a systematic separation of inner and outer regions for the treatment of electron-core coupling problems.[8] We also assumed that applying the orthogonality condition would provide the higher partial waves in the core region; if enough accurate core states were used for the orthogonalization, this statement could

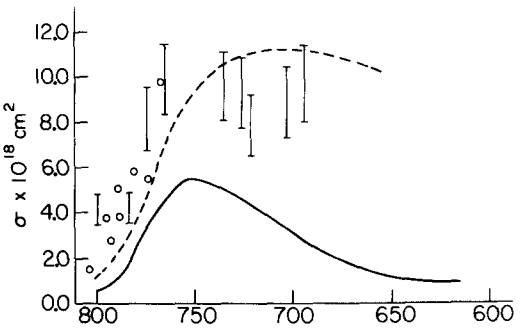

FIG. 1. Direct photoionization cross section of H_2. Experimental: O, Cook and Metzger (Ref. 12); I, Wainfan *et al.* (Ref. 11); theoretical: - - -, Flannery and Opik (Ref. 2); —, present calculation..

be made as nearly accurate as one desired. Hence our accuracy in the core region is essentially limited by the truncation of the set to which we orthogonalize Ψ. This is a parallel to the situation in a linear variational calculation, in which the truncation error arises in the limited choice of expansion functions.

The Schrödinger equation for the system has the form,

$$\begin{aligned}
\text{A:}\ & -(2/R^2)(\lambda^2-\mu^2)^{-1}\{(\lambda_2^2-1)(\partial^2/\partial\lambda^2) \\
& +2\lambda_2(\partial/\partial\lambda_2)+(1-\mu_2^2)(\partial^2/\partial\mu_2^2)-2\mu_2(\partial/\partial\mu_2) \\
& +[(\lambda_2^2-1)^{-1}+(1-\mu_1^2)^{-1}](\partial^2/\partial\varphi^2)+2R\lambda_2\}\psi(2) \\
\text{B:}\ & +\{E_0-E+\langle 0\,|\,r_{12}^{-1}\,|\,0\rangle\}\psi(2), \\
\text{C:}\ & \pm\{(2E_0-E)\langle 0\,|\,\psi\rangle+\langle 0\,|\,r_{12}^{-1}\,|\,\psi\rangle\}\Phi_0(2)=0.
\end{aligned} \tag{7a}$$

The terms labeled A constitute the principal homogeneous parts of the equation and B and C are the Coulombic and exchange parts, respectively.

The equation for each jth component of $\psi(2)$ takes the form,

$$\begin{aligned}
\text{A}\ :& -(2/R^2)\{[(\lambda^2-1)(\partial^2/\partial\lambda^2)+2\lambda(m+1)(\partial/\partial\lambda) \\
& +m(m+1)+2R\lambda+(1-\mu^2)(\partial^2/\partial\mu^2) \\
& -2\mu(\partial/\partial\mu)]F\}_j \\
\text{B:}\ & +[(\lambda^2-\mu^2)(E^0-E+\langle 0\,|\,r_{12}^{-1}\,|\,0\rangle)F]_j \\
\text{C:}\ & \pm\{[(\lambda^2-\mu^2)/(\lambda^2-1)^{m/2}][(2E_0-E)\langle 0\,|\,\psi\rangle \\
& +\langle 0\,|\,r_{12}^{-1}\,|\,\psi\rangle]\Phi\}_j=0.
\end{aligned} \tag{7b}$$

We let the subscript j indicate projection onto the jth harmonic $P_j^m(\mu)$ by premultiplication and integration, in the usual way. The positive and negative signs for term C correspond to triplet and singlet states.

The coupled equations (7b) are truncated to the few strongly coupled terms and are solved by the method of Marriott and Percival.[26] The boundary conditions, in addition to the usual condition that the wavefunction be bounded, included the cusp conditions, the requirement that the wavefunction and its first and second derivatives remain finite at the nuclei. Integration was carried out by a Milne predictor–corrector method, after a short Runge–Kutta start. Details of the calculation are presented elsewhere.[27]

The functions $\Psi(1, 2)$ obtained by this method are already useful for determining energy eigenvalues, in the case of bound state functions, or for giving phase shifts, in the case of continuum functions. However, for our purposes, correct core behavior is important. This was obtained by orthogonalizing our $^1\Sigma_u$ and $^1\Pi_u$ Ψ functions to the first excited state functions of these symmetries. The first excited $^1\Sigma_u$ and $^1\Pi_u$ functions were those computed by Browne, who supplied these functions to us, for a wide range of internuclear distances R.[28] Browne's functions are multiconfiguration functions expanded in the form of Eq. (6).

The autoionization rates were computed as they were by Berry and Nielsen,[5] with the electronic factor,

$$F_{i,f}(R)=(\epsilon_i-\epsilon_f)^{-1},\ \int\psi_f^*(\partial/\partial R)\psi_i d\mathbf{r}, \tag{8a}$$

acting as the kernel of the transition amplitude

$$T_1=\int_0^\infty \chi_i(R)F_{i,f}(R)\frac{\partial\chi_f}{\partial R}\,dR. \tag{8b}$$

The vibrational functions χ were those computed by Berry and Nielsen, with a Numerov integration over a close analytic fit to the H_2^+ function of Bates, Ledsham, and Stewart.[29] Equations (8a) and (8b) were integrated by seven-point quadrature.

III. RESULTS AND DISCUSSION

A. Direct Ionization

The results of the orthogonalization to Ψ_b^i are the first we examine. Table I gives the dipole matrix element for direct photoionization to the $^1\Sigma_u^+$ and $^1\Pi_u$ continuum states for several energies. Projecting out the bound function apparently does not change the wavefunction drastically from these results.

The direct contribution to the total photoionization cross section is shown in Fig. 1, together with the experimental results of Cook and Metzger[14] and of Wainfan, Walker, and Weissler,[13] and the theoretical results of Flannery and Öpik.[2] The model of Flannery and Öpik was based on a Weinbaum ground state function, and a continuum function obtained by integrating the Schrödinger equation with a potential due to two point charges, each with $\frac{1}{2}$ e unit of charge, at a distance chosen to give the correct quadrupole moment for H_2^+. In our treatment and that of Flannery and Öpik, the direct photoexcitation was obtained in the neighborhood of the equilibrium internuclear distance of H_2, because the transitions observed for H_2 are primarily from the ground vibrational state.

The angular distribution is conveniently expressed in terms of the parameter a/b, if the differential cross section $\sigma(\Omega)$ is written as $a+b\cos^2\theta$. Alternatively, $\sigma(\Omega)$ is sometimes written as $[\alpha+\beta P_2(\cos\theta)]$, in which case β/α becomes the useful parameter. Table II shows the values of a/b and β/α obtained from this work, the values reported previously,[7] which were computed from the dipole moments of Flannery and Öpik,[2] and the phase shifts of Temkin and Vasavada.[23] Recent experimental measurements by Carlson and Jonas[30] give a value of a/b for H_2 of 0.048 at the wavelength of the helium resonance line, 585 Å, and 0 ± 0.037 at the 736,744 Å Ne line.

B. Autoionization

The autoionizing states and other states lying above the ionization limit contribute to the total absorption

TABLE II. Angular dependence of $\sigma(\theta)=a+b\cos^2\theta=\alpha+\beta P_2(\cos\theta)$.

	Tully *et al.* Ref. 6		This work		
λ(Å)	a/b	β/α	a/b	β/α	Ref. 25 a/b
800	0.051	1.735	0.071	1.650	
780	0.051	1.735	0.068	1.660	
760	0.051	1.735	0.067	1.667	
740	0.050	1.740	0.065	1.674	0.0 ± 0.037
720	0.050	1.740	0.063	1.683	
700	0.050	1.740	0.060	1.698	
680	0.049	1.742	0.058	1.702	
660	0.049	1.742	0.055	1.719	
640	0.048	1.748	0.053	1.730	
620	0.048	1.748	0.051	1.735	
600	0.047	1.750	0.050	1.740	0.048
580	0.046	1.759	0.048	1.748	
560	0.045	1.760	0.046	1.759	

oscillator strength but, for the most part, yield no fluorescence. The quasibound states that do not autoionize presumably predissociate, because both autoionization and predissociation are generally far faster than radiation. Berry and Nielsen examined the competition between vibrationally induced autoionization and predissociation to states with attractive potential wells. Their results have been our guide for apportioning decay processes between the two channels. We are now in a position to examine the various modes of excitation and decay for H_2, excited by light in the region λ800–600 Å.

First, we have examined the total absorption oscillator strength, per unit of energy, in the manner of Fano and Cooper.[31] Fano and Cooper pointed out that this function is continuous across the ionization threshold and is generally smooth everywhere. Figures 2 and 3 show the total electronic oscillator strength per unit energy for the $^1\Sigma_u^+\leftarrow{}^1\Sigma_g^+$ and $^1\Pi_u\leftarrow{}^1\Sigma_g^+$

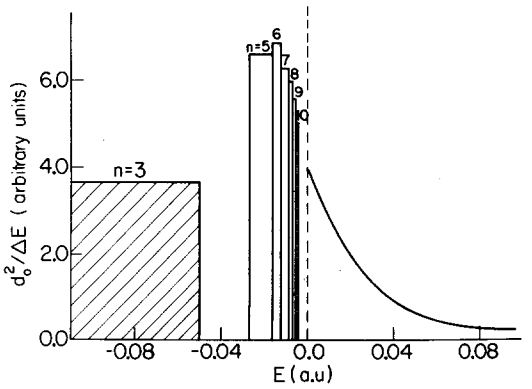

FIG. 2. Oscillator strength (axial component) as a function of energy. Here we have plotted $d_0^2/\Delta E$, a quantity proportional to (df/dE), as a function of E. The histogram at negative energies represents values for Σ bound states $np\sigma\,{}^1\Sigma_u$, while the continuum at positive energies represents ionized $kp\sigma$ states. Areas under the curves represent total electronic oscillator strength; this has not been spread out according to any rotational or vibrational distribution. The intent here is to show the continuity of this function from bound to continuum states, as well as to show the importance of various energy regions in dipole absorption (including ionization).

transitions. No spreading associated with vibrations and rotations has been included. (Hatched portions were computed by Rothenberg and Davidson[32]; there is a blank at $n=4$ in Fig. 2 because the intensity of this transition has not been calculated or measured.) Clearly, the continuity rule applies very well.

The net contribution of Rydberg states to ionization falls faster with increasing energy than their contribution to absorption because both processes, excitation and ionization from the Rydberg state, depend as n^{-3} on the principal quantum number n of the Rydberg state, and the net rate is given approximately by the product of the two rates. The high Rydberg states may also decay via radiation or collisions before they autoionize. Hence it is not surprising that the photoionization curves of Berkowitz and Chupka exhibit very little structure for $\lambda<700$. The alternative is

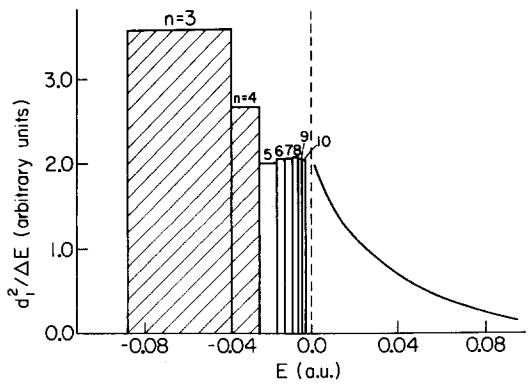

FIG. 3. Oscillator strength (nonaxial component) as a function of energy.

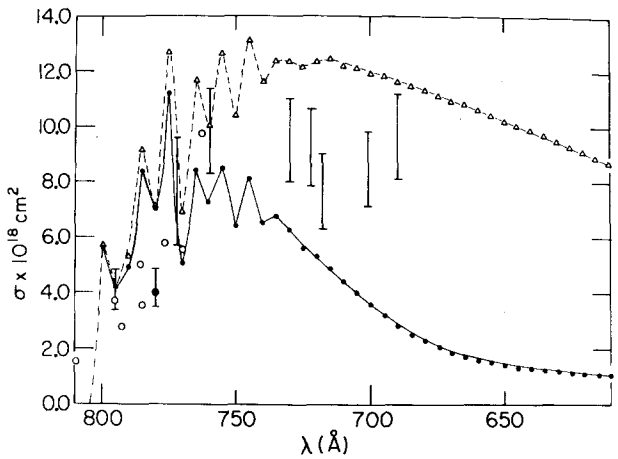

FIG. 4. Total photoionization cross section of H_2. Experimental: O, Cook and Metzger (Ref. 12); I, Wainfan *et al.* (Ref. 11); theoretical: - - -, Flannery and Opik (Ref. 2); —, present. The theoretical curves are obtained by adding the predicted autoionization cross section of the present calculation to the direct calculations quoted.

possible in principle, but unlikely, that there are very many sharp autoionizing states contributing to the total ionization in the region of ~700 Å, and that these states are simply unresolvable.

If we assume that there are no autoionizing contributions for $\lambda < 750$ Å, we can construct a "low-resolution" curve of the total ionization cross section. This is shown in Fig. 4, together with the same experimental data given in Fig. 1. The autoionizing states included in this figure are the $np\sigma$, π, with $6 \leq n \leq 10$. The intensities associated with direct and autoionizing transitions, in the region from the ionization threshold at 804–700 Å, are given in Table III.

The next level of results is the assignment of specific peaks in the photoionization spectrum. We have considered only transitions of para-H_2, from the initial state $v''=0$, $j''=0$, which means, effectively, the $R(0)$ transitions observed with cold H_2.[10–12] For this purpose, it was necessary to compute the wavelengths of specific rotational lines. Table IV gives the observed wavelengths and frequencies of lines in the photoionization spectrum[10–12] and the frequencies calculated for transitions to autoionizing states. The table includes most of the peaks in the photoionization spectrum in the region 801–745 Å,[12] and the assignments of these lines by Takezawa,[16] by Chupka and Berkowitz,[12] and by ourselves. (We have also included four assignments by Herzberg and Jungen,[18] whose results very recently came to our attention.) We have only included Rydberg states with $n \geq 7$, since there are apparently relatively few problems in assigning the $R(0)$ lines of states of lower n, and their autoionization rates are relatively low. The predicted frequencies are systematically low by 20–100 cm^{-1}, with an average deviation of 60 cm^{-1} for $29R(0)$ lines with n between 7 and 10. The discrepancies for $n=6$ are similar, but vary between 100 and 250 cm^{-1} for the assigned $5p\pi R(0)$ lines. In both the $n\sigma$ and the $n\pi$ series, the theoretical frequencies are close enough to the observed frequencies in the absorption spectrum and differ in such a systematic way, that we may have considerable confidence in using the theoretical frequencies to assign peaks in the photoionization spectrum. There are some seven $R(0)$ transitions that were not assigned in the published results of Chupka and Berkowitz,[12] for which we have learned that our assignments are in agreement with tentative but unpublished assignments of Chupka and Berkowitz. Furthermore one can try to interpret the shapes or, as in the present context, the widths of the peaks in terms of lifetimes due to vibrationally induced autoionization.

Certain assignments deserve some comment. Chupka and Berkowitz assign the $9\sigma_3$ $R(0)$ line at 129 300 cm^{-1} or 773.4 Å, overlapping the $6\sigma_4 R(0)$ line. This assignment gives a discrepancy between the experimental and theoretical values of 108 cm^{-1}, roughly twice that for the other $n\sigma_3$ lines, and a distinct deviation of +65 cm^{-1} in the 3–2 vibrational spacing, and of about −50 cm^{-1} in the 4–3 spacing, which suggest that

TABLE III. Integrated intensities of direct and autoionizing contributions to total photoionization of H_2 from 804 to 700 Å. The table gives

$$\int_{804}^{\lambda_0} \sigma(\lambda) d\lambda$$

as a function of the upper limit of the integral, in units of $cm^2 \times 10^{26}$.

λ_0(Å)	Direct contribution	Autoionizing contribution
804	0	0
800	4.8	23.2
795	9.2	36.4
790	13.2	59.1
785	25.4	89.1
780	36.5	97.9
775	56.7	133.2
770	74.9	140.8
765	95.3	161.5
760	119	174
755	144	192
750	169	199
745	195	214
740	220	221
735	246	229
730	265	237
725	293	241
720	316	245
715	337	249
710	356	251
705	374	253
700	390	255

TABLE IV. Experimental and theoretical $R(0)$ lines in the spectrum of H_2. Upper value is the theoretical frequency, lower frequency is experimental, and the experimental wavelength is the third figure. (T) refers to Ref. 15; (CB) to Ref. 11. Lines without parenthetic identification were identified by us and then found to agree with tentative but unpublished assignments by Chupka and Berkowitz. Theoretical uncertainties are about 15 cm^{-1}, from the computations themselves. the theoretical $7p\sigma_1$ and $7p\pi_1$ levels are below the ionization threshold.

$np\sigma$ $n \backslash v$	1	2	3	4	5
7	...	126 305	128 200	130 015	131 725
	124 305.1(T)	126 356.6(T)	128 271(CB)[d]	130 115(CB)	...
		791.45	779.6	768.60	
8	124 780	126 900	128 775	130 610	132 315
	124 867.7(T)	126 917.5(T)	128 830.9(T)	unobserved	132 433(CB)
	800.86	787.90	776.21	(pred. 765.4)	755.06
9	125 185	127 300	129 190	131 000	132 705
	125 242.8(T)	127 314.6(T)	129 299(CB)	131 070(CB)	132 749(CB)
	798.46	785.4	773.4	762.98	753.34
10	125 465	127 580	129 475	131 295	133 005
	125 515.4(T)	127 599.0(T)[c]	129 516(CB)	131 328(CB)	132 996(CB)
	796.7	783.7	772.1	761.44	751.76
$np\pi$					
7	...	126 530	128 430	130 250	131 950
	124 508.8(T)	126 557.7(T)	128 485(CB)	130 310	...
	803.2	790.15	778.3	767.4	...
8	124 920	127 045	128 925	130 745	132 450
	125 017.9(T)	127 064.4(T)	129 007(CB)	130 800	...
	799.90	786.97	775.15	764.55	...
9	125 280	127 400	129 290	131 105	132 810
	125 419.2(T)[a]	127 437	129 374	...	...
	797.35	784.7	772.95	(no autoionizing feature at 131, 180±25)	
10	125 545	127 660	129 545	131 325	133 075
	125 652[b]	127 680	129 635–40	...	...
	795.85	783.2	771.35–40	...	...

[a] Assigned as a mixture of states dominated by $6p\sigma_2$ according to Herzberg and Jungen (Ref. 18 and private communication). These authors assign the $9p\pi_1$ to 125 356.9 cm^{-1}.

[b] $Q(1)6p\pi_2$, according to Herzberg and Jungen; they assign $R(0)$ $10p\pi_1$ to 125 638.6 cm^{-1}.

[c] $10p\sigma_2$ (but with σ and π mixed by l coupling and a good quantum number of $N = 0$) is assigned to 127 572.2 cm^{-1} by Herzberg and Jungen; they attribute its shift to interaction with $5p\sigma_4$ at 127 599.4 cm^{-1}.

[d] $7p\sigma_3$ does not appear in the absorption spectrum because of destructive interference with $5p\sigma_4$ (128 249.8 cm^{-1}) and $14p(N=2)$, at 128 263.0 cm^{-1}, according to Herzberg and Jungen. It would lie at about 128 286 cm^{-1}, were it to be detectable.

either the upper state of the $9\sigma_3$ line is perturbed upward by another state, or that the assignment of $9\sigma_3$ should be made to the weak long-wave shoulder of the 129 300 cm^{-1} line or to the 129 257 cm^{-1} line (773.65 Å), currently assigned as the $4\pi_6$. We believe that perturbation by the $6\sigma_4$ state is the most probable explanation for the shift, and that the high intensity of the line at 773.4, in both absorption and photoionization, is probably due to constructive interference of the transition dipoles of the $9\sigma_3$ and $6\sigma_4$ excitation processes. If this is the case, then there is presumably another state, with a very small transition dipole, located at about 129 180 cm^{-1}, which is also roughly a 50–50 mixture of $9\sigma_3$ and $6\sigma^4$ with phases giving destructive interference. The perturbation parameter (the off-diagonal element of the Hamiltonian) must be about 60 cm^{-1}, and the zero-order states must be nearly degenerate for this perturbation. Previous calculations of Rydberg states and their couplings[33] had not indicated that these two states in particular would couple; the model of Berry and Nielsen indicated that $6\sigma_4$ would interact with $8\sigma_3$, $5\sigma_5$, and $4\sigma_7$, and that the $6\pi_4$ and $9\pi_3$ would interact with each other. The experimental results and the calculations presented

here show that, with their errors in energies of a few hundred cm^{-1}, the previous calculations are, in fact, not accurate enough to be used to predict specific state couplings. (This is in accord with the caveat given by Berry and Nielsen.[33])

Another example of an apparent perturbation is the line at 130 115 cm^{-1} (768.55 Å), tentatively assigned as $7\sigma_4$ by Chupka and Berkowitz.[12] In the same frequency region are the $14\sigma_3$ and $15\sigma_3$ lines. The theoretical calculation, with its presumed systematic error of 30–60 cm^{-1} for the $v=4$ lines, would place the transition at about 130 014 cm^{-1}, so that we would expect the unperturbed $7\sigma_4$ line at about 130 040–130 070 cm^{-1}. There is a relatively strong line at 768.8 Å (130 073 cm^{-1}) assigned "tentatively" as $14\sigma_3$. We presume that this ionization and absorption is actually due to a mixture of $14\sigma_3$ and $7\sigma_4$, with constructive interference occurring for the lower-energy mixed state at 130 073 and destructive interference occurring for the 130 115 cm^{-1} lines.

The $8\sigma_4$ line is predicted by theory to fall at about 130 608, so that one would look for it at about 130 660 cm^{-1}. No such transition is to be seen in either the photoionization or absorption spectrum. In this particular case, the excited bound $8\sigma_4$ state appears to fall within about 40–60 cm^{-1} of the ionization threshold for $H_2^+(v=3)$, and on the high energy side of this threshold. Our predicted autoionization rate τ^{-1} for the $8\sigma_3$ is 1.2×10^{12} sec^{-1}, corresponding to a width $\tau^{-1}/2\pi c$ of about 64 cm^{-1}. Given the near resonance of the $8\sigma_4$ state of H_2 and the $v=3$ state of H_2^+, it would not be surprising if the coupling were somewhat stronger than our "golden rule" calculation indicates. It is quite reasonable to suppose that the $8\sigma_4R(0)$ line is simply too broad to be detected, either in absorption or in photoionization.

The $7\sigma_5$ and $13\sigma_4$ lines seem to be another strongly interacting pair, with only one mixed state giving rise to a detectable line at about 758.85 Å.

The $9\pi_4$ and $10\pi_4$ transitions appear to be missing altogether. This could be due to rapid autoionization; the predicted rate is 1.2×10^{13} for the $9\pi_4$ and 3.0×10^{12} for $10\pi_4$, but the predicted decay rate for $8\pi_4$ is 2.5×10^{12}, clearly too fast for the line at 764.55 to which it is assigned. We therefore must remain skeptical about the validity of our predicted decay rates for the $n\pi$ series and try to explain the problematical $9\pi_4$ and $10\pi_4$ lines on another basis. The $9\pi_4$ may be mixed with some other state to give the line at 761.95 Å (131 242 cm^{-1}), which is somewhat stronger than the $8\pi_4$ and falls about 50 cm^{-1} higher in energy than one would expect the $9\pi_4$ to lie. In the case of the $10\pi_4$, the situation is a little more difficult to rationalize. The $3\pi_{12}$ and $5\pi_6$ states are close by and might be involved in mixing.

Our analysis assigns the broad line in photoionization at 744.75 Å (134.275 cm^{-1}) as the $9\sigma_6R(0)$ line. (The prediction is 744.57 Å or 134 305 cm^{-1}.) The $9\sigma_7$ is predicted at 135 415 cm^{-1} or 738.5 Å. The $10\sigma_5R(0)$ line is predicted at 133 000 cm^{-1} or 751.85 Å, and a peak to which we make this assignment appears[11] at 751.75 Å. Finally, the $10\sigma_6R(0)$ transition is predicted at 134 595 cm^{-1} or 742.97 Å; we have learned[34] that there is a peak at about 742.8 Å with about $\frac{2}{3}$ the height of the $9\sigma_6$ line at 944.75 Å. We shall say more about this particular group of lines in the next section.

Finally, we may mention the $8\sigma_5$ line, assigned tentatively by Chupka and Berkowitz as the strong, broad peak in the photoionization spectrum at 775.1 Å (132 433 cm^{-1}). Both our calculations and the apparent preference of Chupka and Berkowitz place the $8\sigma_5$ line at an energy just *below* the threshold for formation of $H_2^+(v'=4)$. The peak at 755.1 Å, however, is just *above* the threshold, which lies at approximately 775.2 Å. Here we may well have a case of a broad state that actually overlaps the edge of a continuum. In this case, a zero-order model would say that the low-energy side of the line could only autoionize via a $\Delta v=-2$ process, while the high-energy side could autoionize by a $\Delta v=-1$ process. This naive picture is not consistent with the notion of a homogeneously broadened line or with the symmetrical shape that the line appears to have[12]; we can only say at this stage that the shape of such a line remains to be studied.

The calculated autoionization rates of several states are shown in Table V, together with rates calculated from linewidths measured by Berkowitz and Chupka.[12] In a few instances, particularly in the $np\pi$ series, our calculated rates are higher than the widths of the experimental lines. Unfortunately, the higher lines in the π series, especially $n=9$ and 10 lines, are too weak (or broad) to be measured. (Jungen informs us that the higher $np\pi$ lines are not broad; they are weak as a result of l uncoupling, as analyzed by Herzberg and Jungen.[18]) This is apparently the first instance in which a theoretical rate for a vibrationally induced autoionization is faster than the observed rate. In general, the rates calculated here are in slightly better agreement with the rates from experimental linewidths than are those of Berry and Nielsen, which themselves were a marked improvement over the earlier values.[3,4]

One very important point remains to be studied by experiment, the rate of autoionization of the $n\sigma_g$ states. One type of theoretical treatment[3,4] bases its mechanism on coupling of the Rydberg electron to the continuum via the oscillating quadrupole moment of the core, while the other line of approach, into which the present work falls, places the largest part of the coupling on the oscillation of the finite-radius monopole part of the short-range potential of the core.[5] If the $n\sigma_g$ states of low l were simply classifiable as $ns\sigma_g$ and $nd\sigma_g$, then the quadrupole model would predict that the d series would be reasonably broad, similar

TABLE V. Theoretical and experimental rates of autoionization in the $np\sigma$ and $np\pi$ $R(0)$ series of H_2.

			Autoionization rates			
n	v'	Δv	Reference 5	Reference 6	This work	Experimental (Ref. 11)
$np\sigma$ states						
7	2	−2	1.9(9)	6.8(7)	1.8×1(9)	
	3	−2	3.3(9)	3.0(7)	1.1×1(10)	
	4	−2	8.7(9); 1.7(12) for $\Delta v=-1$[a]	3.8(7); 1.1(12) for $\Delta v=-1$	4.6(10)	9.0(11)
	5	−2	2.0(10)	8.2(8)	1.4(11)	
	6	−2	4.0(10)		3.6(11)	
	7	−2			6.4(11)	
8	1	−1	2.1(11)	1.1(11)	3.7(11)	4.0(11)
	2	−1	4.8(11)	2.7(11)	7.6(11)	1.3(12)
	3	−1	7.9(11)	4.8(11)	1.1(12)	2.7(12)
	4	−2(obs,−1)	5.8(9); 1.1(12) for $\Delta v=-1$[a]	2.5(7); 7.4(11) for $\Delta v=-1$	2.7(10)	
	5	−2	1.3(10); 1.6(12) for $\Delta v=-1$[a]	5.5(8); 1.1(12) for $\Delta v=-1$	7.2(10)	2.0(12)
	6	−2	2.7(10)		1.8(11)	
	7	−2			3.3(11)	
9	1	−1	1.5(11)[a]		4.9(11)	3.0(11)
	2	−1			8.6(11)	
	3	−1			1.0(12)	
	4	−1	8.1(11)	5.2(11); 1.8(7) for $\Delta v=-2$	4.2(11)	2.7(12)
	5	−1, −2	1.1(12)	5.8(12); 4.0(8) for $\Delta v=-2$	3.5(11)	5.8(12)
	6	−1, −2			2.2(12)	>9(11)[b]
	7	−1, −2			3.8(12)	
10	1	−1			2.3(11)	
	2	−1			4.3(11)	
	3	−1			6.8(11)	
	4	−1	5.8(11)		7.0(11)	2.0(12)
	5	−1, −2	8.0(11)		6.4(11)	1.7(12)
	6	−1, −2			6.3(11)	
	7	−1, −2			8.3(11)	
$np\pi$ states						
7	2	−2	8.7(8)		2.6(9)	
	3	−2	3.0(9)		2.7(10)	
	4	−2	7.9(9)		1.7(11)	
	5	−2	1.7(10)		5.8(11)	
	6	−2	3.6(10)		1.7(12)	
	7	−2			2.8(12)	
8	1	−1	1.9(11)	1.1(11)	1.0(12)	3.0(11)
	2	−1	4.2(11)		2.0(12)	9.0(11)
	3	−1	7.0(11)		3.1(12)	2.0(12)
	4	−1	1.0(12)		2.5(12)	
	5	−2	1.3(10)		4.5(11)	
	6	−2	2.5(10)		1.6(12)	
	7	−2			2.8(12)	
9	1	−1	1.4(11)	8(10)	7.6(11)	
	2	−1	3.0(11)		2.5(12)	
	3	−1	4.9(11)		4.4(12)	
	4	−1	7.4(11)		1.2(13)	
	5	−1	1.0(12)		3.9(13)	
	6	−1	1.3(12)		8.3(13)	
	7	−1			7.1(13)	

TABLE V (*Continued*)

			Autoionization rates			
n	v'	Δv	Reference 5	Reference 6	This work	Experimental (Ref. 11)
$np\pi$ states						
10	1	−1			6.5(11)	
	2	−1			1.4(12)	
	3	−1			2.3(12)	
	4	−1			3.0(12)	
	5	−1			3.7(12)	
	6	−1			4.1(12)	
	7	−1			3.9(13)	

[a] Based on n^{-3} scaling law.
[b] Our measurement, from Ref. 13.

to the p series, but that the s series would be very sharp because there can be no $J=0\rightarrow J=0$ transitions induced by any multipole higher than the monopole. The finite multipole model, by contrast, implies high autoionization rates for $ns\sigma_g$ states, just because it includes a finite monopole. The problem is complicated by the fact that the real $n\sigma_g$ adiabatic states are not pure $ns\sigma_g$ or $nd\sigma_g$ states, but are mixtures that "switch" from virtually pure s to nearly pure d (or d to s) in the vicinity of the equilibrium internuclear distance.[35,36] In the states of high n, this switching is restricted to a very narrow interval within the nuclear vibration, so that one may expect that, for sufficiently high n, the motion will be diabatic and switching will be inhibited. Hence one would expect the $n\sigma_g$ states to tend toward one sharp s-like series and one broad d-like series, with increasing n, if the quadrupolar model were correct; if, on the other hand, the finite monopole coupling were dominant, no such separation into sharp and broad series would occur. Unfortunately, the $n\sigma_g$ states are not accessible from the ground state of H_2 by optical spectroscopy and probably can only be produced for such a study by electron impact or some very highly selective electron capture process by H_2^+, for example, or by two-photon spectroscopy.

C. Photoelectron Spectroscopy

Energy analysis of the photoelectrons from H_2 was first used by Doolittle and Schoen to show that the energy distribution of the photoelectrons from an autoionizing state is markedly different from the energy distribution of photoelectrons associated with direct ionization.[37] Berkowitz and Chupka[11] pursued this phenomenon by using a tunable light source; they were able to resolve individual $R(0)$ lines in the spectrum of H_2 and then resolve the photoelectron energies well enough to determine the relative proportion of electrons associated with different changes in the vibrational energy of the H_2^+ core associated with autoionization. The results showed that transitions with $\Delta v=-1$ are generally much more probable than those with $\Delta v=-2$, in accordance with the propensity rule suggested by one of us.[3] Transitions involving Δv larger than about -3 apparently do not always satisfy this role, because such transitions, being very improbable, depend on details of the noncancelling parts of nearly vanishing integrals over vibrational wave functions.

The present work revealed a potentially interesting situation that lends itself to direct tests by photoelectron spectroscopy. In contrast to the usual situation in which the propensity role is obeyed, the $9\sigma_5$, $9\sigma_6$, $10\sigma_5$, and $10\sigma_6R(0)$ lines are predicted by the present calculations to gain significant portions of their width by processes in which $\Delta v=-2$. We therefore make specific predictions regarding the energies of the photoelectrons produced when the excited states of these lines autoionize and, more important, regarding the relative numbers of electrons having various energies.

The $9\sigma_5R(0)$ line falls at 753.3 Å or 132 749 cm^{-1}. (The predicted wavelength is 753.56Å, and the corresponding frequency is 132 700 cm^{-1}.) Electrons associated with a $\Delta v=-1$ transition leave with 0.03 eV; those from a $\Delta v=-2$ transition leave with 0.26 eV. The calculated decay rates for these two processes are 9.1×10^{10} and 2.6×10^{11}, respectively. In this case, theory predicts the ratio of faster ($\Delta v=-2$) electrons to slower ($\Delta v=-1$) electrons to be 2.8:1, *favoring the faster electrons.*

The $9\sigma_6R(0)$ line is predicted at 744.57 Å or 134 306 cm^{-1}; a broad line occurs at 744.74 Å or 134 275 cm^{-1}, which is probably this line. Alternatively, a *very* broad feature seems to be present in the photoionization spectrum at about 744.3 Å or 134 354 cm^{-1}, which might be $9\sigma_6$. If the line at 744.74 Å is responsible, then the photoelectrons from $\Delta v=-1$ and $\Delta v=-2$ processes have energies of 0.01 and 0.22 eV, respec-

tively; if the broad feature at 744.3 Å is the $9\sigma_6$, then the photoelectron energies are both 0.01 eV higher. The decay rates are 1.06×10^{12} and 2.23×10^{12} for $\Delta v=-1$ and $\Delta v=-2$ processes, respectively, so that the fast electrons should be in a ratio of 0.47:1 to the slow electrons. Here the $\Delta v=-1$ process is only slightly favored.

The $10\sigma_5R(0)$ line is predicted at 751.86 Å (133 003 cm^{-1}) and observed at 751.75 Å (133 023 cm^{-1}). The slow electrons should have energies of 0.07 eV from a $\Delta v=-1$ process, and the fast electrons, 0.29 eV from a $\Delta v=-2$ process. The *slow* electrons should predominate, in a ratio of about 5.8:1, due to the decay rates of 5.6×10^{11} and 9.5×10^{10} for $\Delta v=-1$ and -2 processes, respectively.

The $10\sigma_6R(0)$ line is predicted to fall at 743.0 Å, and a feature probably attributable to this line falls at about 742.8 Å.[34] The slow electrons coming from autoionization of $10\sigma_6$ should have energies of 0.05 eV and the fast electrons, energies of 0.26 eV, due to $\Delta v=-1$ and -2 processes. The rates of decay for -1 and -2 processes are 3.3×10^{11} and 2.9×10^{11} sec^{-1}, so that the ratio of numbers of slow-to-fast electrons should be only about 1.1:1.

In summary, we infer the following: (a) The correlated pseudopotential method, or orthogonalization to correlated core functions of a reasonably accurate function calculated with Coulomb and exchange as we have done, gives eigenvalues of sufficient accuracy to be useful for spectroscopic purposes. (b) This method gives reasonably reliable values for electronic transition probabilities to Rydberg states and continuum states near the ionization threshold. (c) The introduction of correlation, in H_2 at least, has only a small effect on the dipole matrix elements we have studied, and on the predicted angular distribution of photoelectrons. We are thereby encouraged to use methods without correlation to get moderately accurate pictures of photoionization cross sections and angular distributions in more complex species. It is now clearly possible to examine quantitatively the distribution of oscillator strength among the decay modes of direct ionization and (presumably) dissociation, of autoionization and of predissociation. (d) Rates of autoionization of the $np\sigma$ states are given reasonably well by theory. Experimental data are insufficient to provide a critical test for the $np\pi$ series, although the available experimental and theoretical data are in reasonable agreement. (e) It is now possible to predict relative intensities for photoelectron spectra, in order to test the reliability of calculations of relative rates of different autoionization processes from a given quasibound state.

ACKNOWLEDGMENTS

This work was supported by the National Science Foundation, Grant GP-10547. We would like to thank Dr. Herzberg and Dr. Jungen for supplying us with a copy of their manuscript prior to publication and for their comments. We would also like to thank Dr. John Tully for his comments.

* Present address: Department of Chemistry, University of Illinois, Urbana, Ill.

[1] M. J. Shimizu, J. Phys. Soc. Japan **15,** 1440 (1960).
[2] M. R. Flannery and U. Öpik, Proc. Phys. Soc. (London) **86,** 491 (1965).
[3] R. S. Berry, J. Chem. Phys. **45,** 1228 (1966).
[4] A. Russek, M. R. Patterson, and R. L. Becker, Phys. Rev. **167,** 17 (1968).
[5] R. S. Berry and S. E. Nielsen, Phys. Rev. A **1,** 395 (1970).
[6] F. H. Faisal, Phys. Rev. A **4,** 1396 (1971).
[7] J. Tully, R. S. Berry, and B. J. Dalton, Phys. Rev. **176,** 95 (1968).
[8] U. Fano, Phys. Rev. A **2,** 353 (1970).
[9] G. Herzberg, Phys. Rev. Letters **23,** 1081 (1969).
[10] W. A. Chupka and J. Berkowitz, J. Chem. Phys. **48,** 5726 (1968).
[11] J. Berkowitz and W. A. Chupka, J. Chem. Phys. **51,** 2341 (1969).
[12] W. A. Chupka and J. Berkowitz, J. Chem. Phys. **51,** 4244 (1969).
[13] N. Wainfan, W. C. Walker, and G. L. Weissler, Phys. Rev. **99,** 542 (1955).
[14] G. R. Cook and P. H. Metzger, J. Opt. Soc. Am. **54,** 968 (1964).
[15] F. J. Comes and H. O. Wellern, Z. Naturforsch. **23a,** 881 (1968).
[16] S. Takezawa, J. Chem. Phys. **52,** 2575 (1970).
[17] S. Takezawa, J. Chem. Phys. **52,** 5793 (1970).
[18] G. Herzberg and Ch. Jungen, J. Mol. Spectry. (to be published).
[19] J. C. Tully, Phys. Rev. **181,** 7 (1969).
[20] J. C. Tully and R. S. Berry, J. Chem. Phys. **51,** 2056 (1969).
[21] R. W. Ditchburn and U. Öpik, in *Atomic and Molecular Processes,* edited by D. R. Bates (Academic, New York, 1962).
[22] P. G. Burke and A. J. Taylor, Proc. Phys. Soc. (London) **88,** 549 (1966).
[23] A. Temkin and J. C. Lamkin, Phys. Rev. **121,** 788 (1961).
[24] A. Temkin and K. V. Vasavada, Phys. Rev. **160,** 109 (1967).
[25] J. C. Tully and R. S. Berry, J. Chem. Phys. **51,** 2056 (1969).
[26] R. Marriott, Proc. Roy. Soc. (London) **A78,** 121 (1958).
[27] G. B. Shaw, Doctoral thesis, University of Chicago, Chicago, Ill., March 1971.
[28] J. C. Browne, J. Chem. Phys. **40,** 43 (1964); (also private communication).
[29] D. R. Bates, K. Ledsham, and A. L. Stewart, Phil. Trans. Roy. Soc. (London) **A246,** 215 (1953).
[30] T. A. Carlson and A. E. Jonas, J. Chem. Phys. **55,** 4913 (1971).
[31] U. Fano and J. W. Cooper, Rev. Mod. Phys. **40,** 441 (1968).
[32] S. Rothenberg and E. R. Davidson, J. Mol. Spectry. **22,** 1 (1967).
[33] R. S. Berry and S. E. Nielsen, Phys. Rev. A **1,** 383 (1970).
[34] W. A. Chupka (private communication).
[35] S. E. Nielsen and R. S. Berry, Phys. Rev. A **4,** 865 (1971).
[36] B. Andresen and S. E. Nielsen, Mol. Phys. **21,** 523 (1971).
[37] P. H. Doolittle and R. I. Schoen, Phys. Rev. Letters **14,** 348 (1965).